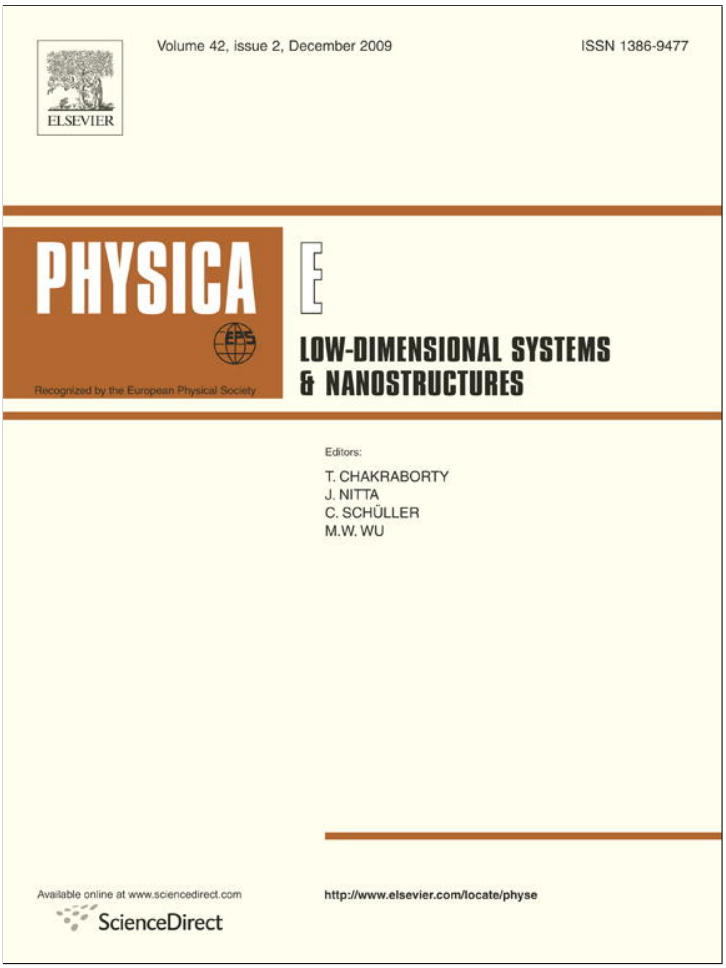

Physica E 42 (2009) 104–109

Contents lists available at ScienceDirect

Physica E

journal homepage: www.elsevier.com/locate/physe

Vibrating carbon nanotube based bio-sensors

R. Chowdhury *, S. Adhikari *, J. Mitchell

School of Engineering, Swansea University, Singleton Park, Swansea SA2 8PP, UK

ARTICLE INFO

Article history:
Received 4 June 2009
Received in revised form
7 September 2009
Accepted 17 September 2009
Available online 23 September 2009

PACS:
61.46.Fg
73.63.Fg
68.65.Hb

Keywords:
Nanotube
Mass sensor
Finite element simulation
Frequency-shift

ABSTRACT

The potential of single-walled carbon nanotubes (SWCNTs) as a mass sensor is examined using continuum mechanics based approach. The carbon nanotube resonators are assumed to be either in cantilevered or in bridged configurations. Simple analytical formulas are developed for CNT-based nanoresonators with attached mass. A closed-form expression has been derived to detect the mass of biological objects from the frequency-shift. A simple linear approximation of the nonlinear sensor equation has been investigated. The validity and the accuracy of these formulas are examined for a wide range of cases. The results indicate that the new sensor equations can be used for CNT-based biosensors with reasonable accuracy.

1. Introduction

Since their discovery [1,2] in 1991, carbon nanotubes (CNTs) have received much attention as a new class of nanomaterials [3,4]. They have unique physical properties [5–8], which leads to variety of applications in many different fields such as scanning probes [9,10], nanoelectronics, storage devices [11–14] and nanoelectromechanical systems. Nanotubes have been utilized as nanoactuators [15], nanosensors [7,8,16] and electrochemical sensing system [17–21]. The use of vertically aligned single-walled carbon nanotube (SWCNTs) for field emission and vacuum microelectronic devices, and as nanosensors and nanoactuators, is being actively explored [22,23].

There has been a growing interest of CNTs in biological applications [24–26,13,27], especially in medical technology [28] and sensors [7,8] which can be broadly classified into two categories [29,30]: chemical sensors [31] and biosensors [32–34]. The application of CNTs have been explored for the development of ultrasensitive nano-bio sensors [26,13], electro-analytical nanotube devices [27] and electromechanical actuators for artificial muscles [35]. The development of nano-bio sensors [36] and nanoscale bioreactor systems based on CNTs has been driven by the experimental evidence that biological entities such as proteins, enzymes, bacteria can be immobilized either in the hollow cavity or on the surface of carbon nanotubes [24,25]. Significant attempts are being made for the use of CNTs as superior biosensor materials in the light of successful fabrication of various electroanalytical nanotube devices, modified by external biological agents [35,37–39]. These devices, prepared as SWCNT transistors, have shown promising sensitivities required for such applications as antigen recognition [37], enzyme-catalyzed reactions [38], and DNA hybridizations [39].

Resonance based sensors offer the deeper potential of achieving the high-fidelity requirement of many sensing applications. The principle of mass detection using resonators is based on the fact that the resonant frequency is sensitive to the resonator mass, which includes the self-mass of the resonator and the attached mass. The change of the attached mass on the resonator causes a shift to the resonant frequency. The key issue of mass detection is in quantifying the change in the resonant frequency due to the added mass. In the present study, we explore the potential of using SWCNTs as nanomechanical resonators in nanosized mass sensors. Simple analytical formulae are derived for cantilevered and bridged SWCNTs with attached mass, representing the relation between the resonant frequency of a CNT resonator and the attached mass. For the analysis of resonant frequency of CNT resonators, we adopt the continuum mechanics method, which is combined with commercial finite element (FE) software.

* Corresponding authors. Tel.: +44 1792 602088; fax: +44 1792 295676.
E-mail addresses: R.Chowdhury@swansea.ac.uk (R. Chowdhury), S.Adhikari@swansea.ac.uk (S. Adhikari).
URLS: http://engweb.swan.ac.uk/~chowdhuryr/ (R. Chowdhury), http://engweb.swan.ac.uk/~adhikaris (S. Adhikari).

1386-9477/$ - see front matter © 2009 Elsevier B.V. All rights reserved.
doi:10.1016/j.physe.2009.09.007

2. Resonant frequencies of SWCNT with attached mass

The continuum models based on beam as well as shell have been used extensively for single- and multi-walled carbon nanotubes, see for example [40–48]. In order to obtain simple analytical expressions of the mass of attached biochemical entities, we model a single-walled CNT using a rod based on the Euler–Bernoulli beam theory [23]. The equation of motion of free-vibration can be expressed as

$$EI\frac{\partial^2 y}{\partial x^2}+\rho A\frac{\partial^2 y}{\partial t^2}=0 \tag{1}$$

where E is Young's modulus, I the second moment of the cross-sectional area A, and ρ the density of the material. Suppose the length of the SWCNT is L. Depending on the boundary condition of the SWCNT and the location of the attached mass, the resonant frequency of the combined system can be derived. We only consider the fundamental resonant frequency, which can be expresses as

$$f_n=\frac{1}{2\pi}\sqrt{\frac{k_{eq}}{m_{eq}}} \tag{2}$$

Here k_{eq} and m_{eq} are respectively equivalent stiffness and mass of SWCNT with attached mass in the first mode of vibration. Two kinds of end constraints, i.e., cantilever and bridged, are considered. As shown in Fig. 1, for the cantilevered resonator, the additional mass is assumed to be attached in the free end. For bridged resonator, the additional mass is assumed to be attached in the middle of nanotube length as shown in Fig. 2.

2.1. Cantilevered SWCNT with mass at the tip

Suppose the value of the added mass is M. As shown in Fig. 1, we give a virtual force at the location of the mass so that the deflection under the mass becomes unity. For this case it can be shown that [49] $F_{eq}=3EI/L^3$ so that

$$k_{eq}=\frac{3EI}{L^3} \tag{3}$$

The deflection shape along the length of the SWCNT for this case can be obtained as

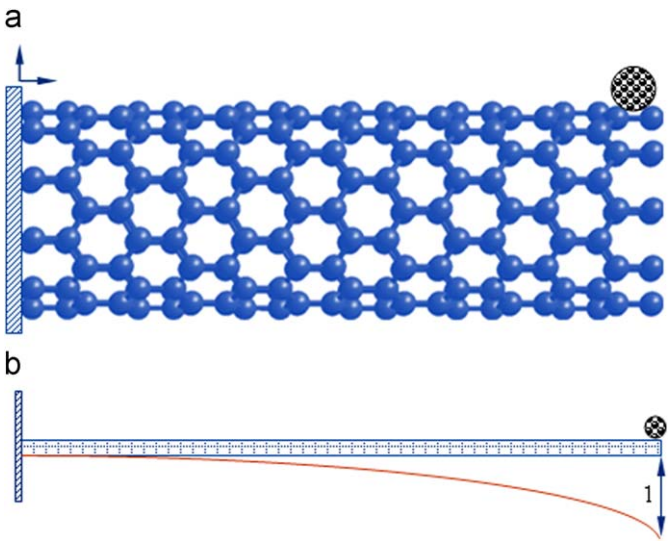

Fig. 1. Cantilevered nanotube resonator with an attached mass at the tip of nanotube length. (a) Original configuration; (b) mathematical idealization. Unit deflection under the mass is considered for the calculation of kinetic energy of the nanotube.

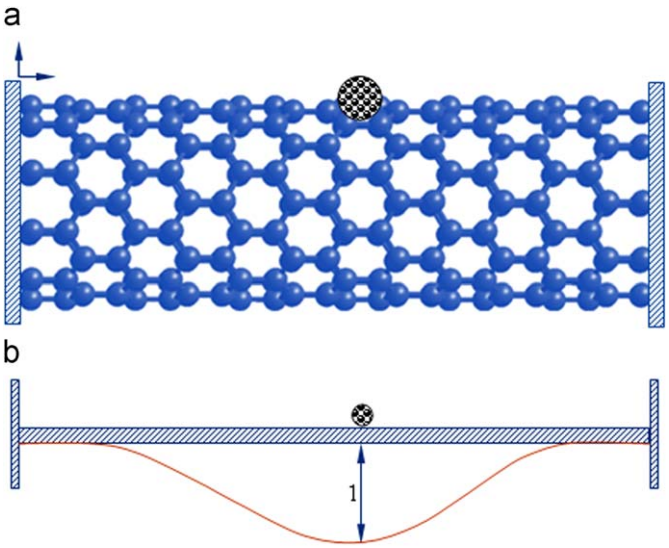

Fig. 2. Bridged nanotube resonator with an attached mass at the center of nanotube length. (a) Original configuration; (b) mathematical idealization. Unit deflection under the mass is considered for the calculation of kinetic energy of the nanotube.

$$Y(x)=\frac{x^2(3L-x)}{2L^3} \tag{4}$$

Assuming harmonic motion, i.e., $y(x,t)=Y(x)\exp(i\omega t)$, where ω is the frequency, the kinetic energy of the SWCNT can be obtained as

$$T=\frac{\omega^2}{2}\int_0^L \rho AY^2(x)dx+\frac{\omega^2}{2}MY^2(L)=\rho A\frac{\omega^2}{2}\int_0^L Y^2(x)dx + \frac{\omega^2}{2}M1^2=\frac{\omega^2}{2}\left(\frac{33}{140}\rho AL+M\right) \tag{5}$$

Therefore

$$m_{eq}=\frac{33}{140}\rho AL+M \tag{6}$$

The resonant frequency can be obtained using Eq. (2) as

$$f_n=\frac{1}{2\pi}\sqrt{\frac{k_{eq}}{m_{eq}}}=\frac{1}{2\pi}\sqrt{\frac{3EI/L^3}{\frac{33}{140}\rho AL+M}} =\frac{1}{2\pi}\sqrt{\frac{140}{11}}\sqrt{\frac{EI}{\rho AL^4}}\sqrt{\frac{1}{1+\frac{M}{\rho AL}\frac{140}{33}}}=\frac{1}{2\pi}\frac{\alpha^2\beta}{\sqrt{1+\Delta M}} \tag{7}$$

where

$$\alpha^2=\sqrt{\frac{140}{11}}\quad\text{or}\quad\alpha=1.888 \tag{8}$$

$$\beta=\sqrt{\frac{EI}{\rho AL^4}} \tag{9}$$

and

$$\Delta M=\frac{M}{\rho AL}\mu,\quad \mu=\frac{140}{33} \tag{10}$$

Clearly the resonant frequency for a cantilevered SWCNT with no added tip mass is obtained by substituting $\Delta M=0$ in Eq. (7) as

$$f_{0_n}=\frac{1}{2\pi}\alpha^2\beta \tag{11}$$

Combining Eqs. (7) and (11) one obtains the relationship between the resonant frequencies as

$$f_n = \frac{f_{0_n}}{\sqrt{1+\Delta M}} \tag{12}$$

2.2. Bridged SWCNT with mass at the midpoint

This case is shown in Fig. 2. Again we give a virtual force at the location of the mass so that the deflection under the mass becomes unity. For this case it can be shown that [49] $F_{eq} = 192EI/L^3$ so that

$$k_{eq} = \frac{192EI}{L^3} \tag{13}$$

The deflection shape along the length of the SWCNT can be obtained as

$$Y(x) = \begin{cases} \frac{32}{L^3}(1/2x^3 - 3/8x^2L), & x < L/2 \\ \frac{32}{L^3}(1/2x^3 - 3/8x^2L - (x-1/2L)^3), & x \geq L/2 \end{cases} \tag{14}$$

Assuming harmonic motion, the kinetic energy of the SWCNT can be expressed by

$$T = \frac{\omega^2}{2}\int_0^L \rho A Y^2(x)dx + \frac{\omega^2}{2}MY^2(L) = \frac{\omega^2}{2}\left(\frac{13}{35}\rho AL + M\right) \tag{15}$$

The first integral was calculated by splitting the integral into two parts and choosing the appropriate expressions of $Y(x)$ from Eq. (14). The equivalent mass is

$$m_{eq} = \frac{13}{35}\rho AL + M \tag{16}$$

The resonant frequency can be obtained using Eq. (2) as

$$f_n = \frac{1}{2\pi}\sqrt{\frac{192EI/L^3}{\frac{13}{35}\rho AL + M}} = \frac{1}{2\pi}\frac{\alpha^2\beta}{\sqrt{1+\Delta M}} \tag{17}$$

where β is given by Eq. (9) and

$$\alpha^2 = \sqrt{\frac{6720}{13}} \quad \text{or} \quad \alpha = 4.768 \tag{18}$$

and

$$\Delta M = \frac{M}{\rho AL}\mu, \quad \mu = \frac{35}{13} \tag{19}$$

These equations are now used to obtain the mass based on the frequency-shift.

3. General derivation of the sensor equations

In this section we derive a general expression of the added mass of bio-particles based on the frequency-shift of the SWCNT. The frequency-shift can be expressed using Eq. (12) as

$$\Delta f = f_{0_n} - f_n = f_{0_n} - \frac{f_{0_n}}{\sqrt{1+\Delta M}} \tag{20}$$

From this we obtain

$$\frac{\Delta f}{f_{0_n}} = 1 - \frac{1}{\sqrt{1+\Delta M}} \tag{21}$$

Rearranging gives the expression

$$\Delta M = \frac{1}{\left(1 - \frac{\Delta f}{f_{0_n}}\right)^2} - 1 \tag{22}$$

This equation completely relates the change is mass frequency-shift. Expanding Eq. (22) in Taylor series one obtains

$$\Delta M = \sum_j (j+1)\left(\frac{\Delta f}{f_{0_n}}\right)^j, \quad j = 1, 2, 3, \ldots \tag{23}$$

Therefore, keeping up to first and third order terms one obtains the linear and cubic approximations as

$$\Delta M \approx 2\left(\frac{\Delta f}{f_{0_n}}\right) \tag{24}$$

and

$$\Delta M \approx 2\left(\frac{\Delta f}{f_{0_n}}\right) + 3\left(\frac{\Delta f}{f_{0_n}}\right)^2 + 4\left(\frac{\Delta f}{f_{0_n}}\right)^3 \tag{25}$$

The general relationship between the frequency-shift and added mass of bio-particles in a SWCNT is shown in Fig. 3. The exact relationship in Eq. (22) is compared with the linear and cubic approximations in Eqs. (24) and (25) respectively. The actual value of the added mass can be obtained from Eq. (22) as

$$M = \frac{\rho AL}{\mu}\frac{(\alpha^2\beta)^2}{(\alpha^2\beta - 2\pi\Delta f)^2} - \frac{\rho AL}{\mu} \tag{26}$$

Using the linear approximation, the value of the added mass can be obtained as

$$M = \frac{\rho AL}{\mu}\frac{2\pi\Delta f}{\alpha^2\beta} \tag{27}$$

As shown in the previous section, the nondimensional constant α depends on the boundary conditions and μ depends on the location of the mass. For a cantilevered SWCNT with a tip mass $\alpha^2 = \sqrt{140/11} = 3.5675$, $\mu = 140/33 = 4.2424$ and for a bridged SWCNT with a mass at the midpoint $\alpha^2 = \sqrt{6720/13} = 22.7359$, $\mu = 35/13 = 2.6923$. The forms of Eqs. (26) and (27) will remain the same for other boundary configurations. The only changes will be in the numerical values of the constants α and μ.

4. Finite element modeling

In this study a single-walled carbon nanotube is modeled using a 3D solid finite element structural analysis [51] model under FEMLAB environment [50]. The FE model of CNT and bacteria,

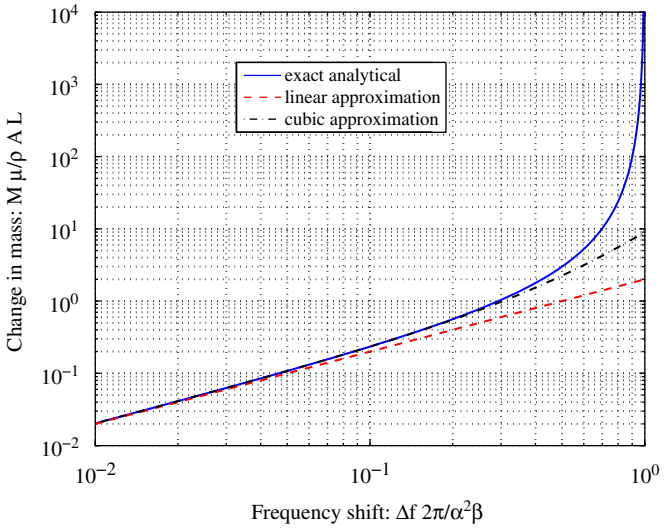

Fig. 3. The general relationship between the normalized frequency-shift and normalized added mass of the bio-particles in an SWCNT with effective density ρ, cross-section area A and length L. Here $\beta = \sqrt{EI/\rho AL^4}\,s^{-1}$, the nondimensional constant α depends on the boundary conditions and μ depends on the location of the mass. For a cantilevered SWCNT with a tip mass $\alpha^2 = \sqrt{140/11}$, $\mu = 140/33$ and for a bridged SWCNT with a mass at the midpoint $\alpha^2 = \sqrt{6720/13}$, $\mu = 35/13$.

shown in Fig. 4, follows hollow circular cylinder and ellipsoidal shape. Following is the mesh statistics of the system: number of degrees of freedom = 55,401, number of mesh point = 2810, number of elements (tetrahedral element) = 10,974, number of boundary elements (triangular element) = 3748, number of vertex elements = 22, number of edge elements = 432, minimum element quality = 0.2382 and element volume ratio = 0.0021. The lengths of carbon nanotubes can differ greatly, ranging from a few nm to microns. It has been reported that CNTs can have a length-to-diameter ratio of up to 28,000,000:1 [52]. Based on this, the finite element model can change significantly. In this study, the chosen length of the nanotube is 8 nm. Geometrical and material properties for both the SWCNT as well the bacterial mass are presented in Table 1.

4.1. Model validation

In order to verify the accuracy of this model, the frequencies obtained are compared with results from a molecular dynamics (MD) simulation study using the same dimensions and material properties [53]. Boundary condition of FE model is taken as clamped both ends. The results are displayed in Table 2. The table identifies that the results are in good agreement with the previous study. This shows a maximum discrepancy between the finite element model and the MD simulation results of approximately 4% for the 8 nm length model. This comparison provides a great deal of confidence for the use of this model in further investigations as a mass sensor.

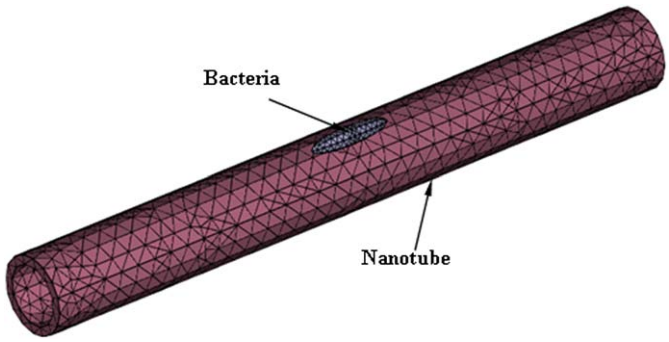

Fig. 4. Finite element simulation model. The theory of linear elasticity is used for both the CNT and the bacteria and the properties used are reported in Table 1. Mesh statistics used for numerical calculations are as follows: number of degrees of freedom = 55,401, number of mesh point = 2810, number of elements (tetrahedral element) = 10,974, number of boundary elements (triangular element) = 3748, number of vertex elements = 22, number of edge elements = 432, minimum element quality = 0.2382 and element volume ratio = 0.0021. Chosen length of the nanotube is 8 nm and length of bacteria is varied between 0.5 to 3.5 nm.

Table 1
Geometrical and material properties for the single-walled carbon nanotube and the bacterial mass.

SWCNT	Bacteria (*E. coli*)
$L = 8$ nm [53]	$E = 25.0$ MPa [54]
$E = 1.0$ TPa [53]	$\rho = 1.16$ g/cc [55]
$\rho = 2.24$ g/cc [53]	–
$D = 1.1$ nm [56]	–
$v = 0.30$ nm	–

Table 2
Comparison of frequencies (100 GHz) obtained from finite element simulation with MD simulation for the bridged configuration. For the 8.0 nm SWCNT used in this study, the maximum error is less than about 4%.

D (nm)	L (nm)		f_1	f_2	f_3	f_4	f_5
1.1	4.1	MD	10.315	10.315	10.478	10.478	15.796
		FE	10.769	10.769	16.859	22.224	22.224
		%error	−4.40	−4.40	−60.90	−112.10	−40.69
	5.6	MD	6.616	6.616	9.143	9.143	11.763
		FE	6.883	6.884	12.237	14.922	14.924
		%error	−4.04	−4.05	−33.84	−63.21	−26.87
	8.0	MD	3.800	3.8	8.679	8.679	8.801
		FE	3.900	3.9	8.659	9.034	9.034
		%error	−2.63	−2.63	−0.23	−4.09	−2.65

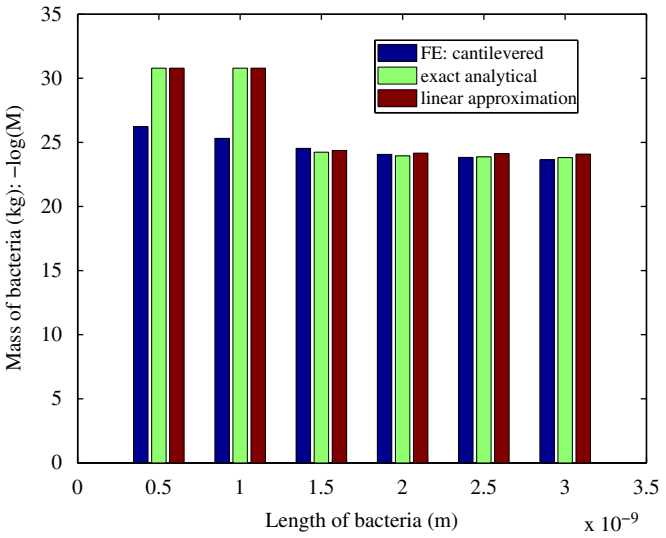

Fig. 5. The variation of identified mass with bacterial length using the finite element simulation, exact analytical formula and the linear approximation for the cantilevered nanotube. Proposed analytical expressions are in good agreement with the detailed finite element results for longer bacterial length.

5. Results and discussion

5.1. Case 1: cantilever nanotube resonator

In this section we verify the accuracy of the proposed sensor-equations derived in Section 3. The fundamental frequency of the SWCNT without any mass was obtained in the previous section. Here we calculated the frequency of the SWCNT with increasing the length of the bacteria and calculate the frequency-shift. The frequency-shift obtained using the finite element method is treated as that obtained from a real experiment. From this 'measured' frequency-shift, the mass of the bacteria is recalculated as if it were unknown. The expressions given by Eqs. (26) and (27) corresponding to exact and linear approximation are used for the identification of the bacterial mass. The true mass used in the finite-element analysis and those obtained using these two expressions are compared in Fig. 5. It can be seen that the error in the identification of the added mass using analytical expression and its linear approximation decreases as the length of bacteria increases.

5.2. Case 2: bridged nanotube resonator

Similar to cantilever resonator, the fundamental frequency of the system decreases as the length of the bacteria increases. The

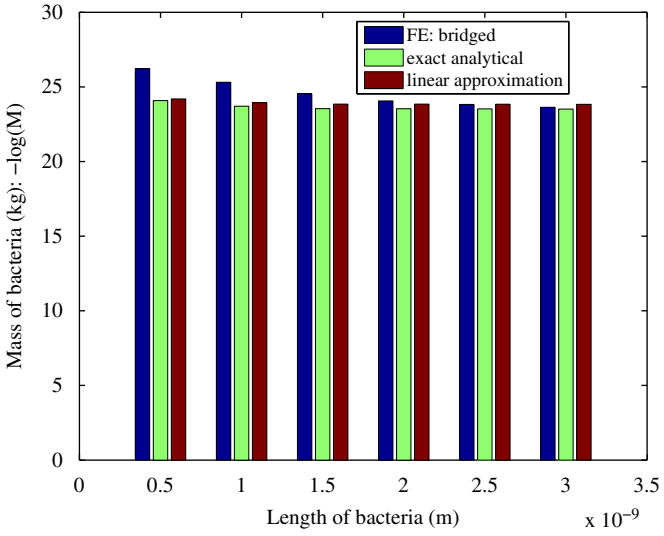

Fig. 6. The variation of identified mass with bacterial length using the finite element simulation, exact analytical formula and the linear approximation for the bridged nanotube. Proposed analytical expressions are in good agreement with the detailed finite element results for longer bacterial length.

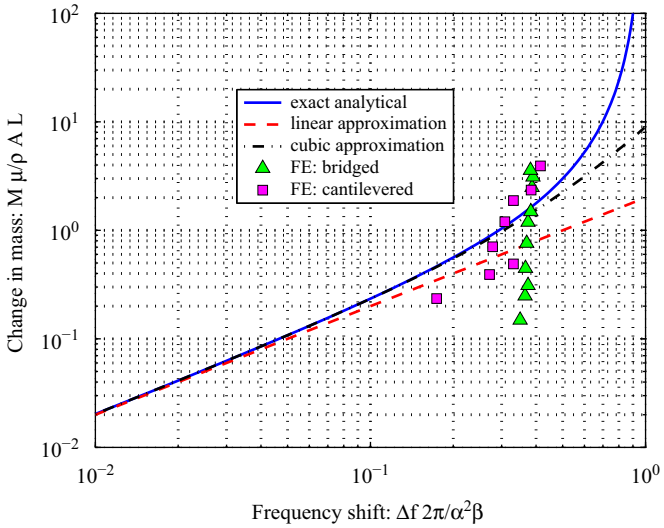

Fig. 7. The general relationship between the normalized frequency-shift and normalized added mass of the bio-particles in an SWCNT with effective density ρ, cross-section area A and length L. Relationship between the frequency-shift and added mass of bio-particles obtained from finite element simulation are also presented here to visualize the effectiveness of analytical formulas.

variation of identified mass with bacterial length using the finite element simulation, exact analytical formula (26) and the linear approximation (27) is shown in Fig. 6. Although the resonant frequencies vary with bacterial length and end constraints, there is a similarity between cantilever and bridged resonator. It is also observed that, variation of the frequency-shift is apparent, when the added mass is larger than 10^{-23} kg. Thus the mass sensitivity of this kind of biosensors can reach at least 10^{-24} kg.

The normalized identified masses for both the cases are summarized and shown in Fig. 7. This plot shows that different configurations can be effectively represented by a single normalized curve. For the examples considered here the normalized frequency-shift is concentrated within a small band. But in many real applications the normalized frequency-shift can be spread-out from 10^{-2} to about 0.75 for the proposed analytical expressions to be applicable.

6. Conclusions

The potential of SWCNT as a mass sensor is explored. CNTs are modeled by continuum based approach. Both cantilevered and bridged CNTs are investigated. The relationship between the resonant frequency and the attached mass is established using the Euler–Bernoulli beam theory. Using this relationship, a general closed-form nonlinear sensor-equation has been derived for the detection of the mass of biological objects attached to the CNT. The physical basis of the sensor is that the attached mass causes a frequency-shift. A simple linear approximation of the nonlinear sensor-equation has been given. The accuracy of both the exact and the linear approximation has been verified using a detailed hi-fidelity finite-element simulation. It was observed that the proposed sensor-equations work reasonably well when the length of the bacteria is more than 1 nm for both cantilevered and bridged configurations. The numerical results indicate that the mass sensitivity of carbon nanotube-based nanobalances can reach up to 10^{-24} kg.

Present results are obtained based on the constant temperature assumption. In practice, temperature fluctuation may influence the vibrational frequency of CNT resonators. This issue needs to be addressed in the future by taking the mechanical as well thermal properties of CNTs.

Acknowledgments

R.C. acknowledges the support of Royal Society through the award of Newton International Fellowship. S.A. gratefully acknowledges the support of UK Engineering and Physical Sciences Research Council (EPSRC) through the award of an Advanced Research Fellowship and The Leverhulme Trust for the award of the Philip Leverhulme Prize.

References

[1] S. Iijima, Nature 354 (6348) (1991) 56.
[2] S. Iijima, T. Ichihashi, Nature 363 (6430) (1993) 603.
[3] M.S. Dresselhaus G.D., Avouris P. (Eds.), Carbon Nanotubes: Synthesis, Structure, Properties and Applications, Springer, Berlin, Germany, 2001.
[4] R. Haddon, Accounts of Chemical Research 35 (12) (2002) 997.
[5] P. Ajayan, Chemical Reviews 99 (7) (1999) 1787.
[6] P. Ajayan, J. Charlier, A. Rinzler, Proceedings of the National Academy of Sciences of the United States of America 96 (25) (1999) 14199.
[7] Y. Lin, et al., Journal of Materials Chemistry 14 (4) (2004) 527.
[8] L. Gu, et al., Chemical Communications (7) (2005) 874.
[9] J. Wang, Electroanalysis 17 (1) (2005) 7.
[10] O. Kumar, et al., Defence Science Journal 58 (5) (2008) 617.
[11] Y. Yun, et al., Nano Today 2 (6) (2007) 30.
[12] G.A. Rivas, et al., Talanta 74 (3) (2007) 291.
[13] R. Baughman, et al., Science 284 (5418) (1999) 1340.
[14] A. Fennimore, et al., Nature 424 (6947) (2003) 408.
[15] C.Y. Li, T.W. Chou, Physical Review B 68 (7) (2003) 3.
[16] C.Y. Li, T.W. Chou, Applied Physics Letters 84 (25) (2004) 5246.
[17] N. Kam, et al., Proceedings of the National Academy of Sciences of the United States of America 102 (33) (2005) 11600.
[18] N.W.S. Kam, H. Dai, Physica Status Solidi B—Basic Solid State Physics, 243 (13) (2006) 3561; 20th International Winterschool/Euroconference on Electronic Properties of Novel Materials, Kirchberg, Austria, March 04–11, 2006.
[19] L. Lacerda, et al., Nano Today 2 (6) (2007) 38.
[20] M. Prato, K. Kostarelos, A. Bianco, Accounts of Chemical Research 41 (1) (2008) 60.
[21] H. Wang, et al., Journal of the American Chemical Society 128 (41) (2006) 13364.
[22] A. Gupta, D. Akin, R. Bashir, Applied Physics Letters 84 (11) (2004) 1976.
[23] D. Wu, et al., Sensors and Actuators A—Physical 126 (1) (2006) 117.
[24] S. Tsang, et al., Journal of the Chemical Society—Chemical Communications (17) (1995) 1803.
[25] J. Davis, et al., Inorganica Chimica Acta 272 (1–2) (1998) 261.
[26] S. Wong, et al., Nature 394 (6688) (1998) 52.
[27] M. Mattson, R. Haddon, A. Rao, Journal of Molecular Neuroscience 14 (3) (2000) 175.

[28] F. Lu, et al., Advanced Materials 21 (2) (2009) 139.
[29] U. Yogeswaran, S. Thiagarajan, S.M. Chen, Sensors 8 (11) (2008) 7191.
[30] U. Yogeswaran, S.M. Chen, Sensors 8 (1) (2008) 290.
[31] J. Wang, M. Musameh, Analytical Chemistry 75 (9) (2003) 2075.
[32] B.L. Allen, P.D. Kichambare, A. Star, Advanced Materials 19 (11) (2007) 1439.
[33] K. Balasubramanian, M. Burghard, Analytical and Bioanalytical Chemistry 385 (3) (2006) 452.
[34] M. Atashbar, et al., in: D. Rocha, P.M. Sarro, M.J. Vellekoop, (Eds.), Proceedings of the IEEE Sensors, vols. 1–3, Vienna, Austria, October 24–27, 2004, pp. 1048–1051.
[35] J. Davis, et al., Chemistry—A European Journal 9 (16) (2003) 3732.
[36] S. Lee, D.S. Yoon, Biochip Journal 1 (3) (2007) 193.
[37] R. Chen, et al., Proceedings of the National Academy of Sciences of the United States of America 100 (9) (2003) 4984.
[38] J. Gooding, et al., Journal of the American Chemical Society 125 (30) (2003) 9006.
[39] J. Li, et al., Nano Letters 3 (5) (2003) 597.
[40] C. Wang, C. Ru, A. Mioduchowski, International Journal of Solids and Structures 40 (15) (2003) 3893.
[41] C. Wang, C. Ru, A. Mioduchowski, Journal of Nanoscience and Nanotechnology 3 (1–2) (2003) 199.
[42] C. Wang, C. Ru, A. Mioduchowski, Journal of Applied Mechanics—Transactions of the ASME 71 (5) (2004) 622.
[43] F. Scarpa, S. Adhikari, Journal of Non-Crystalline Solids 354 (35–39) (2008) 4151.
[44] C. Wang, C. Ru, A. Mioduchowski, Journal of Applied Physics 97 (2) (2005).
[45] C. Wang, C. Ru, A. Mioduchowski, Journal of Applied Physics 97 (11) (2005).
[46] C. Wang, C. Ru, A. Mioduchowski, Journal Computational and Technological Nanoscience 1 (2005) 412.
[47] C. Wang, C. Ru, A. Mioduchowski, Physical Review B 72 (75414) (2005) 1.
[48] F. Scarpa, S. Adhikari, Journal of Physics D: Applied Physics 085306 (2008) 1.
[49] J.E. Shigley, Mechanical Engineering Design, McGraw-Hill, USA, 1988.
[50] W.J. Zimmerman, Multiphysics Modelling with Finite Element Methods, World Scientific, Singapore, 2008.
[51] O.C. Zienkiewicz, R.L. Taylor, The Finite Element Method, fourth ed., McGraw-Hill, London, 1991.
[52] L. Zheng, et al., Nature Materials 3 (10) (2004) 673.
[53] C.Y. Li, T.W. Chou, Applied Physics Letters 84 (1) (2004) 121.
[54] G. Lan, C.W. Wolgemuth, S.X. Sun, Proceedings of the National Academy of Sciences of the United States of America 104 (41) (2007) 16110.
[55] M. Godin, et al., Applied Physics Letters 91 (12) (2007).
[56] C.Y. Li, T.W. Chou, International Journal of Solids and Structures 40 (10) (2003) 2487.